Module-7: Experimental Hypersonic Test facilities and measurements

Lecture-31: Hypersonic wind tunnel

31.1 Hypersonic Test Facilities:

Hypersonic flow is a flow for which speeds are much larger than the local speed of sound. In general hypersonic flow is defined as the flow at Mach 5 or greater at which physical properties of the flow changes rapidly. A test facility designed or considered for hypersonic testing should simulate the typical flow features of this flow regime. These flow features include thin shock layer, entropy layer, viscous interaction and most importantly high total or stagnation temperature of the flow. This section deals with most common facilities for hypersonic testing.

31.2 Continuous Hypersonic Wind Tunnel

Continuous hypersonic wind tunnel is comprised of a compressor, heater, nozzle, test section, diffuser, second throat and vacuum chamber as major components. Schematic of such tunnel is as shown in **Fig.31.1**. During the experimental testing, continuous operation can be achieved by providing continuously operating compressors. Such high pressure air is then heated in the heater so as to reach the desired stagnation temperature. Valve is then operated if sufficient low pressure is attained in the vacuum chamber. Expansion of the air through the convergent divergent nozzle sets the hypersonic flow in the test section. Onwards deceleration of the flow through the second throat ensures the low speed air at the compressor inlet.

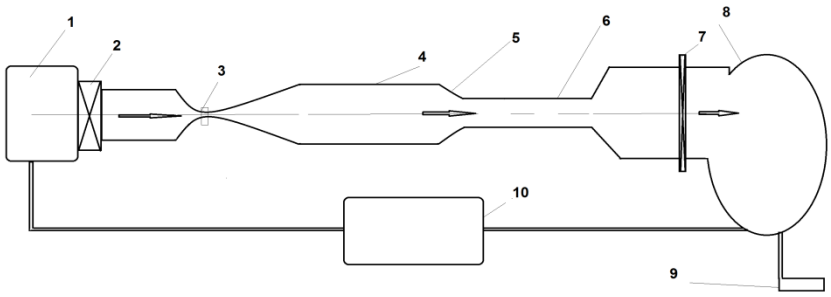

1. Heater 2.Valve 3.First Throat 4.Test section 5.Diffuser 6.Second throat 7.Valve 8.Vacuum Chamber 9.Vacuum pump 10. Multistage compressor

Fig. 31.1: Schematic diagram of continuous hypersonic wind tunnel circuit

31.2.1 Heaters

Condensation free hypersonic expansion of air requires high stagnation temperatures as per the Mach number attained in the test section. In the conventional hypersonic tunnels different types of heater are used to provide the appropriate temperature. The combustion, the electric resistance and the arc-jet type heaters are suitable for continuous or long duration operation. Industrial heaters where air is heated using combustion products are generally preferred up to Mach 8. Resistance wire electric heaters are used to provide for Mach numbers up to 12 to 14. Ceramic materials or special alloys provide support for the heating elements in this heater. Nitrogen is used as the working fluid for high stagnation conditions with direct electric resistance heating because of serious oxidation rates. Direct electric arc heating of the working fluid is used in arc-jet heaters. The moderate stagnation temperatures (<5500° K) for nitrogen freestream are obtained with such type of heaters.

31.2.2 Hypersonic Nozzles

Convergent divergent axi-symmetric nozzles are generally preferred in the hypersonic tunnels. These nozzles expand the high pressure and high temperature air to the desired Mach number in the test section. These nozzles can also be equipped contour to ensure the uniformity of the flow in the test section. The throat of the nozzle needs to be water-cooled for continuous and also for blow-down hypersonic tunnels operating at high stagnation temperatures or high enthalpy conditions. Frequent change of the throat is also encountered for such high enthalpy operations. Beryllium-copper is often used for the throat liners material to provide strength with high heat conductivity. In an alternative design, the throat liner, made of titanium, zirconium and molybdenum alloy, is cooled by working gas (air or nitrogen) before its entry in to the heater.

31.2.3 Hypersonic Diffuser

Typical hypersonic tunnel diffuser is comprised of fixed contraction followed by a constant area diffuser duct. This contraction reduces the flow Mach number. A complex three dimensional shock pattern executes this Mach number reduction. These shock waves interact with the boundary layer during the process. This region is followed by a subsonic flow where deceleration takes place in a divergent section. Diffuser design is very important for the continuous closed circuit wind tunnels due to its dependence on compressor characteristics and drive power. However the design of diffuser for the impulse type facilities is carried out mainly to evaluate the useful test time.

31.3 Blow-down Hypersonic Wind Tunnel

Power requirement of a wind tunnel is directly proportional with the square of the required velocity in the test section. Hence installation of a continuous closed circuit wind tunnel remains a costly affair. In view of this, impulsive experimental facilities like blow-down wind tunnels are designed and installed to simulate the hypersonic flow. This wind tunnel is comprised of major components viz. multi-stage compressor, dryer, heater, settling chamber, nozzle, test section, diffuser and vacuum tank. Schematic of the typical blow-down type wind tunnel is as shown in **Fig. 31.2**. During the operation of the tunnel, air or nitrogen is initially compressed to high pressure using the multistage compressor as per the stagnation pressure requirement. This high pressure fluid is then dried in the dryer to remove the moisture content of the same before it is stored in large tanks. Storage or regenerative type heaters have been developed for application in case of such intermittent or blow-down tunnels. These heaters are essentially insulated pressure vessels. Use of such heaters makes it possible to increase the temperature of the high pressure air but with lower power requirement. The pebbles used in the heaters are mostly refractory ceramic pebbles or cored bricks which are heated using electrical resistance elements or by products of combustion. This high pressure fluid is allowed to pass over a large bed of ceramic pebbles during the experiment. A typical experiment starts after the throttling valve opening due to which the high pressure air passes through the heater and onwards towards to the test section. In some cases a settling chamber is built to provide the high pressure and high temperature reservoir before its expansion in the nozzle.

Expansion of the gas in the nozzle attains the required hypersonic freestream conditions in the nozzle. Higher temperature values of the flow in the test section are preferred to prevent the liquefaction of the air as it expands to very low temperatures in the nozzle.

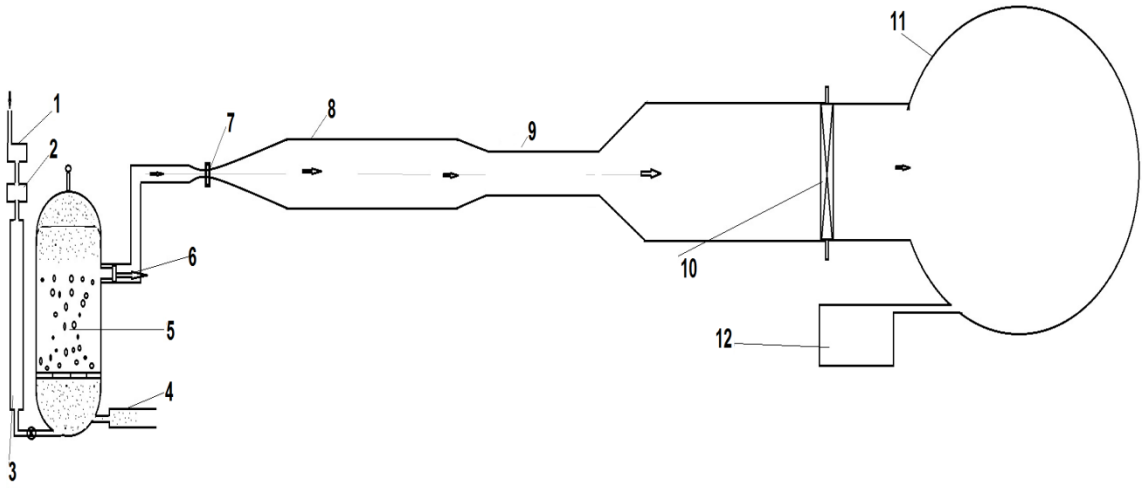

1. Multistage compressor 2.Dryer 3.High pressure air storage 4.Gas inlet 5. Refractory pebbles 6.Start valve 7.Nozzle with throat cooling apparatus 8.Test section 9.Diffuser second throat 10.Valve 11.Vacuum Chamber 12. Vacuum pump

Fig. 31.2: Schematic drawing of the blow-down hypersonic wind tunnel circuit

Lecture-32: Hypersonic wind tunnel and its calibration

32.1 Nitrogen Wind Tunnel

It is a blow-down wind tunnel operated with high pressure Nitrogen gas. Hence the arrangement of this tunnel is same as that of a blow-down wind tunnel (**Fig. 32.1**). The high pressure Nitrogen gas is initially heated by a graphite resistance heater contained within a pressure vessel and then allowed to expand through the nozzle. Experimental duration in these tunnels is in the range of 1 to 4 seconds. Nitrogen wind tunnels also operate between two temperature limits discussed herein. The lower limit on temperature is essentially to avoid condensation effects in the test section, and the upper limit on the temperature is necessarily governed by the heater. Two servo-systems are installed for two reasons viz. controlling the gas flow to maintain a constant stagnation pressure and ensuring a constant current through the heater which effectively controls the stagnation temperature.

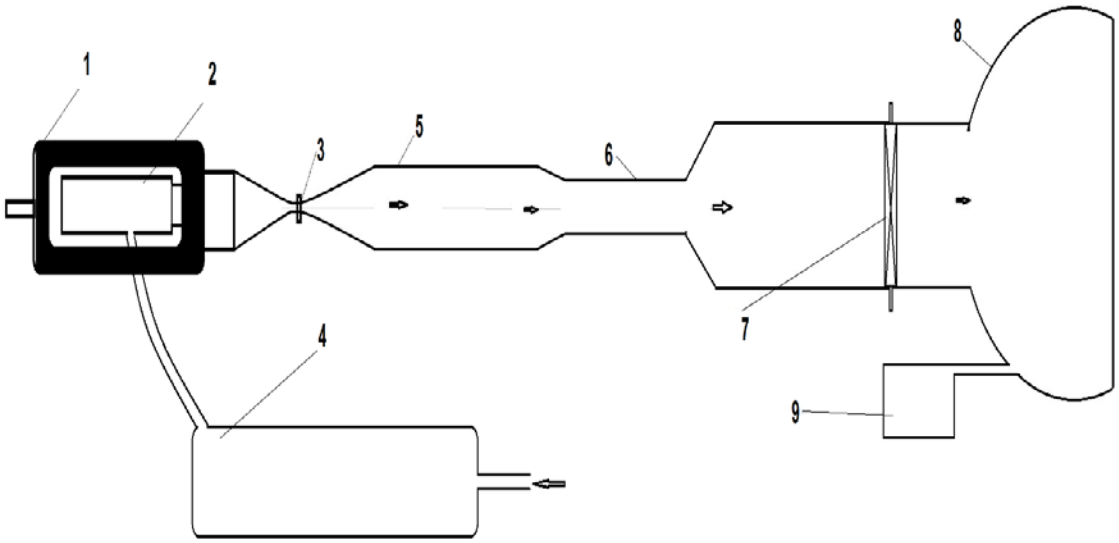

1.High pressure vessel 2.Graphite resistance heater 3.Nozzle with water cooling at throat 4.Multistage compressor 5.Test section 6.Diffuser Second throat 7.Valve 8.Vacuum Chamber 9.Vacuum pump

Fig 32.1: Schematic drawing of Nitrogen wind tunnel circuit

32.2 Continuous Tunnel or Arc Jet Wind Tunnels

This wind tunnel type is used to simulate the hypersonic, hypervelocity and high enthalpy airflows that are experienced by space flights during atmospheric re-entry and also to provide the insight for real gas effect aerodynamics for design of thermal protection system. This tunnel is from the realm of blow-down tunnel where heating of the test gas is carried out using electric heaters. These heaters are placed in the pressure vessel containing high pressure test gas. Copper electrodes with water cooling arrangement are used to enhance the life of the electrode. The high pressure electrically heated test gas is then passed through the convergent divergent nozzle to attain the required Mach number in the test section.

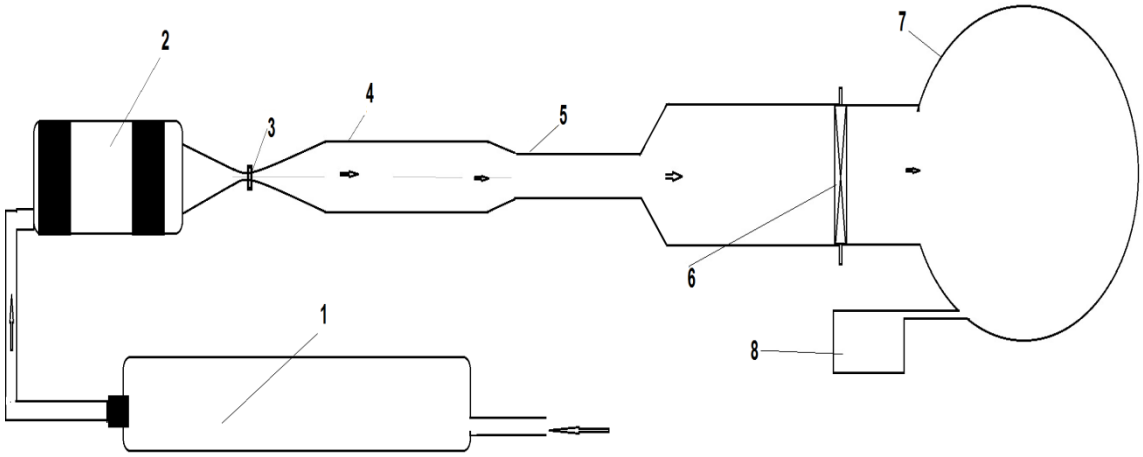

1. Multistage compressor 2. Arc-jet heater 3.Nozzle with water cooling at throat 4.Test section 5.Diffuser Second throat 6.Valve 7.Vacuum Chamber 8.Vacuum pump

Fig. 32.2: Schematic drawing of Arc-Jet wind tunnel circuit

32.3. Flow Parameter Estimations for a Wind Tunnel.

Following techniques can be used to estimate the hypersonic flow parameters in the test section when the wind tunnel is used to simulate the hypersonic Mach number and corresponding Reynolds number.

1. Measurement of Stagnation Pressures: Measure stagnation pressure and stagnation temperature in the settling chamber which is the total pressure ahead of the shock. During the experiments measure the stagnation pressure in the test section using the pitot tube. Ratio of these measured total pressures for assumed constant specific heat ratio provides the freestream Mach number using normal shock relations as given in **Eq. 32.1**.

$$\frac{P_{o2}}{P_{o1}} = \frac{\left[1+\frac{\gamma-1}{2}M_1^{\,2}\right]^{\frac{\gamma}{\gamma-1}}}{\left[1+\frac{\gamma-1}{2}M_2^{\,2}\right]^{\frac{\gamma}{\gamma-1}}}\left[1+\frac{2\gamma}{\gamma+1}\left(M_1^{\,2}-1\right)\right] \qquad (32.1)$$

Thus calculated Mach number and measured total temperature can then be used to evaluate the static temperature in the test section using **Eq. 32.2**.

$$\frac{T_0}{T} = 1+\frac{\gamma-1}{2}M^2 \qquad (32.2)$$

Hence freestream velocity, density and other parameters are then obvious from these calculations.

2. Measurement of Freestream Stagnation and Static Pressures: Measure stagnation pressure and stagnation temperature in the settling chamber which is the total pressure ahead of the shock. During the experiments, measure the static pressure in the test section using the pressure sensor mounted on a flat plate which experiences hypersonic flow at zero degree angle of attack. Ratio of the measured freestream total and static pressures along with the assumed constant specific heat ratio provide the freestream Mach number using isentropic relations.

$$\frac{P_0}{P} = \left[1 + \frac{\gamma - 1}{2} M^2\right]^{\left[\frac{\gamma}{\gamma - 1}\right]} \tag{32.3}$$

Thus calculated Mach number and measured total temperature can then be used to evaluate the static temperature in the test section. Hence freestream velocity, density and other parameters are then obvious from these calculations.

3. Measurement of Freestream Stagnation and Static behind the shock: Measure stagnation pressure and stagnation temperature in the settling chamber which is the total pressure ahead of the shock. During the experiments, measure the static pressure in the test section using the pressure sensor mounted on a flat plate which experiences hypersonic flow at any non-zero degree angle of attack which has the attached shock solution for the given freestream Mach number. Initial guess Mach number of the test gas can be predicted using area ratio of the convergent divergent nozzle of the tunnel.

$$\left(\frac{A}{A^*}\right)^2 = \frac{1}{M^2}\left[\frac{2}{\gamma + 1}\left(1 + \frac{\gamma - 1}{2} M^2\right)\right]^{(\gamma+1)/(\gamma-1)} \tag{32.4}$$

The angle of attack of the plate is chosen using this initial guess Mach number. Ratio of the measured freestream total pressure and static pressures behind the oblique shock along with the assumed constant specific heat ratio provide the freestream Mach number using oblique shock relations. Thus calculated Mach number and measured total temperature can then be used to evaluate the static temperature in the test section. Hence freestream velocity, density and other parameters are then obvious from these calculations.

4. Flow Visualisation for attached oblique shock: Freestream conditions can even be estimated using flow visualisation. For this method, a flat plate has to be mounted in the test section at an angle of attack for which an attached shock solution is expected. Stagnation pressure and temperature of the freestream are to be monitored in the settling chamber. Oblique shock angle will be visualised during the flow visualisation experiments. Known angle of attack of the plate and the oblique shock angle can be used to find out the freestream Mach number under the assumption of constant specific heat ratio using oblique shock relation

$$\tan\theta = 2\cot\beta\left[\frac{M_1^2\sin^2\beta - 1}{M_1^2(\gamma + \cos 2\beta) + 2}\right]$$

Thus calculated Mach number and measured total temperature can then be used to evaluate the static temperature in the test section. Hence freestream velocity, density and other parameters are then obvious from these calculations.

Lecture-33: Hypersonic impulse facilities

33.1 Impulse Test Facilities

There are many experimental facilities (like hypersonic wind tunnels, hypersonic shock tunnels etc.) available around the world to simulate the hypersonic flows. The facilities like wind tunnels are the comparatively long duration facilities, where test time is of the order of few seconds. The power to drive a wind tunnel is directly proportional to cube of the velocity. Although this rule does not hold in case of high-speed flow regimes, the need for rapidly increasing power still remains a fact. Still the simulation of high Mach number flows can be done in long duration test facilities like hypersonic wind tunnels but it is very expensive and difficult to simulate flows with higher energy content in such facilities. Also in the wind tunnels, it is difficult to shift from the conventional test gas (air) to any other test gas. Hence it becomes difficult to simulate the flow conditions in the Martian environment, which is predominantly carbon dioxide. The impulse facilities or short duration test facilities of test duration varying from few tens of microseconds to few milliseconds are invented and designed to reduce the experimental cost and to make it possible to conduct the experiments for hypersonic or hyper-velocity situations. Most of such facilities have their basics in shock tube.

33.2 Shock Tube

The shock tube is a simple tube closed at both ends. A metallic or non-metalic diaphragm is used to divide this duct into two compartments called as driver and driven sections of the shock tube. Driver section is a high pressure section which contains the high pressure gas and that gas. Driven section is a low pressure section which contains the low pressure driven or test gas. In this section pressure transducers are mounted to measure the pressure variation with time at particular location during the experiments. Schematic of a typical shock tube along with the initial pressure distribution is as shown in **Fig. 33.1**

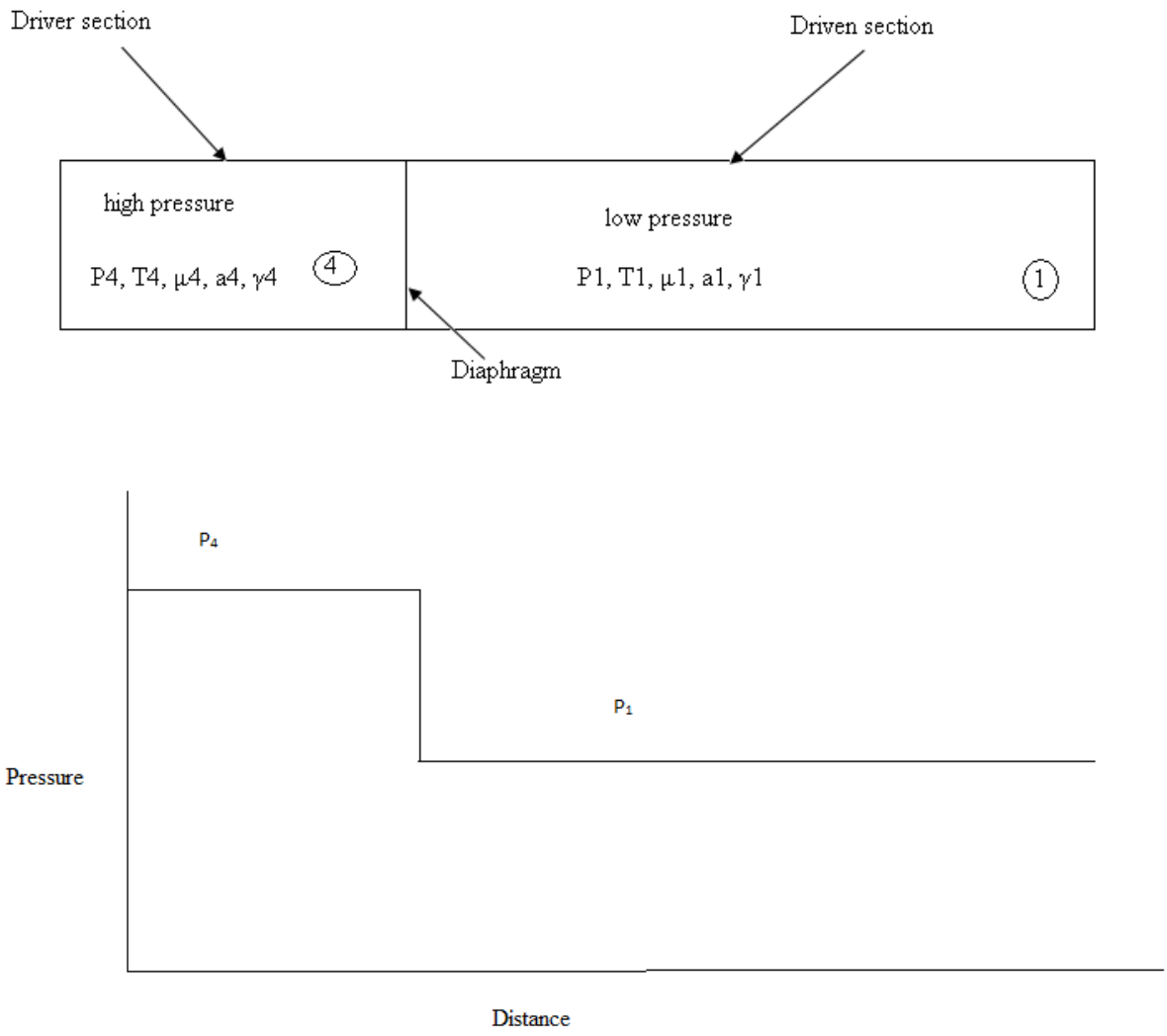

Fig. 33.1. Schematic of a typical shock tube and initial pressure distribution.

During operation of the shock tube, a metallic or non-metallic diaphragm is placed between driver and driven sections. Driven section is then filled with the test gas and then evacuated to a desired lower pressure. Driver section is then continuously filled with the low molecular weight driver gas, till the pressure in this section rises to a value which leads to burst the diaphragm. The diaphragm burst creates compression waves which propagate downstream in the driven section and the expansion waves traversing upstream in the driver section. All the compression waves travelling in the driven section coalesce to form a shock which then travels in the driven section. Travel of this primary shock in the driven section raises the pressure and temperature of the test gas. This increase in pressure can be monitored using pressure sensors mounted in the driven sections. The initial stagnant test gas or driver gas then passes behind the primary shock. The Mach number of this gas depends on the strength of

the shock and can attain supersonic speed in the presence of strong primary shock. Driver gas at the same time undergoes the expansion in the presence of expansion waves. However, the driver and driven gases do not mix in each other due to the presence of contact surface or discontinuity which moves in the driven section behind the primary shock. The pressure and velocity are same across the contact surface. Expansion fan and shock reflect from the closed ends of the shock tube. Reflected shock again passes through the driver gas however it nullifies the momentum making the gas stagnant. Thus driven section end of the shock tube momentarily acts as a reservoir for high temperature and high pressure test gas. The strength of the shock wave and expansion fan thus produced depends on the many parameters viz. initial pressure ratio across the diaphragm, physical properties of the gases in the driver and driven sections, diaphragm thickness etc. The typical space time diagram for the shock in the shock tube is as shown in **Fig. 33.2.**

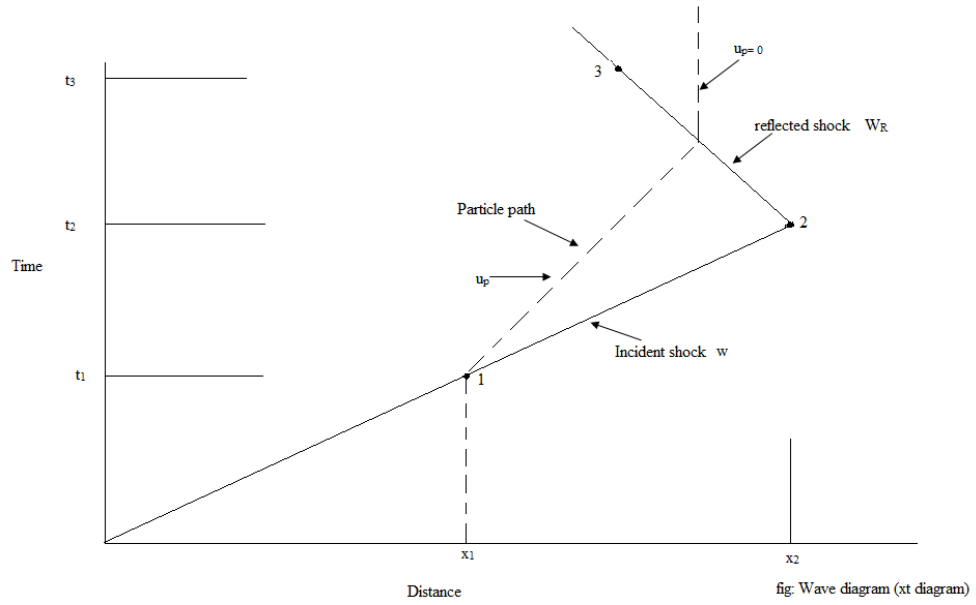

Fig. 33.2 Space time diagram for the shock and particle path for the shock tube

33.3 Diaphragm-less Shock Tube

The above mentioned conventional shock tube has issues related with the operational uncertainties. The main reason of the uncertainty is due to use of diaphragm to operate the shock tube. Change in batch of diaphragm may change the diaphragm material properties, thickness etc. which in turn changes the diaphragm rupture pressure for same experimental conditions. The change in diaphragm rupture pressure changes the primary shock strength and hence the stagnation conditions behind the reflected shock. Hence a mechanism is invariantly thought for to replace the diaphragm of the shock tube to reduce the uncertainty. In view of this a fast acting valve is placed in place of the diaphragm which separates the driver and driven sections of shock tube. Opening of such valve during the experiment operates the shock tube. Rest operation of the diaphragm-less shock tube is same as that of the conventional shock tube.

33.4 Combustion Driven Shock Tube

The shock tube explained earlier is the one where high pressure low temperature driver gas is used to burst the diaphragm. However the strength of the primary shock and hence the reflected shock depends on the temperature of driver gas for given initial driven gas temperature. Hence other derivatives of shock tube are invented to generate higher temperature and pressure at the end of driven end of the shock tube which can then be facilitated in shock tunnel to simulate real gas effects.

Combustion driven shock tube has same configuration as that shown in **Fig. 33.1**.The only difference lies is in the operation of this shock tube. The driver is filled with the air and hydrogen along with the low molecular weight driver gas like helium. Spark plugs are mounted in the driver section to initiate the combustion. Thus started combustion raises pressure and temperature in the driver section which in tern bursts the diaphragm. There onwards the operation of the shock tube is as explained earlier in section 33.2. The increased driver gas temperature helps to increase the shock strength.

Lecture 34: Shock Tunnel and its variants

34.1 Shock Tunnel

A typical shock tunnel is as shown in **Fig. 34.1.** It is very much clear from this figure that, the shock tunnel is an obvious extension of shock tube. A conventional shock tunnel is comprised of three sections viz. shock tube, nozzle and test section dump tank assembly. Nozzle, test section and dump tank together are called as wind tunnel part of the shock tunnel since these parts are similar to that seen in wind tunnel. The driven section end of the shock tube is kept open and connected to the convergent divergent nozzle. The convergent part of the nozzle is provided with minimal length so as to provide the shock reflection. The other end of the nozzle is connected to the test section and dump tank assembly. During the experiment, diaphragm is installed between driver and driven sections of the shock tube. A paper diaphragm is put between the driven section and nozzle. Desired driven or test gas is filled in the driven section and pressure is adjusted using the vacuum pump connected to it. Lowest possible pressure is attainted and then maintained in the test section and dump tank assembly where instrumented test model is mounted. Driver section is then filled with the driver gas till the metallic diaphragm ruptures. Usual shock tube operation persist post diaphragm rupture. The reflected shock provides the high pressure and high temperature test gas at the entry to the nozzle. Further expansion of the test gas in the nozzle attains desired freestream conditions in the test section.

Pressure sensors mounted in the driven section give the pressure rise across the primary shock. Primary shock Mach number can be calculated through measured pressure and known specific heat ratio of the test gas using shock tube relations as,

$$\frac{P_2}{P_1} = \frac{2\gamma\left(M_S\right)^2 - \left(\gamma - 1\right)}{\gamma + 1} \tag{34.1}$$

Here P_1 and P_2 are the pressure ahead and behind the moving primary shock, γ is the specific heat ratio of driver gas and M_s is the primary shock Mach number.

Thus obtained shock Mach number can be used to calculate the pressure and temperature behind the reflected shock as,

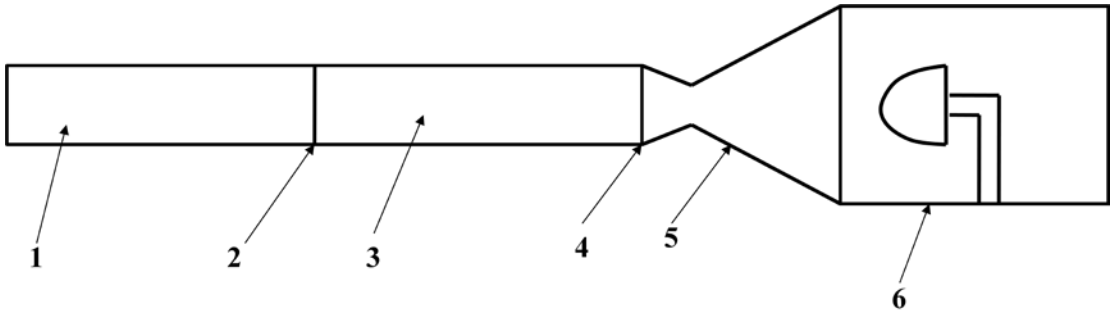

1. Driver Section 2. Diaphragm 3. Driven Section 4.Diaphragm 5.Nozzle 6.Test section and vacuum tank assembly

Fig. 34.1: Schematic of a typical Shock Tunnel

$$\frac{P_5}{P_1} = \left\{ \frac{2\gamma(M_S)^2 - (\gamma - 1)}{\gamma + 1} \right\} \left\{ \frac{(3\gamma - 1)(M_S)^2 - 2(\gamma - 1)}{(\gamma - 1)(M_S)^2 + 2} \right\} \quad (34.2)$$

$$\frac{T_5}{T_1} = \frac{\{2(\gamma - 1)M_s^2 + (3 - \gamma)\}\{(3\gamma - 1)M_s^2 - 2(\gamma - 1)}{2(\gamma + 1)M_s^2} \quad (34.3)$$

Here P_5 and T_5 are the pressure and temperature behind the reflected shock. These properties are necessarily the stagnation properties of the test gas. Flow parameters in the test section can be estimated as discussed in section 32.3. More commonly used method is measurement of pitot pressure (total pressure behind the normal shock) in the test section.

For impulsive type facilities, such as shock tunnels, where extremely high throat heat transfer rate is expected for a short time, it is advisable to provide cooling for the throats. Without any cooling, the throat surface temperature may reach the melting point during a tunnel run and may experience severe oxidation if air is used as the working fluid. Both of these lead to throat erosion, alteration of the throat shape and flow contamination. Therefore, materials such as Tungsten, beryllium oxide may be used to overcome the melting effect in such situations.

34.2 Modifications in Shock Tunnel

Shock tunnels are preferred over the wind tunnel mainly for two reasons viz. cost of operation is low and flows with higher stagnation temperature can be simulated. However the higher stagnation temperature of the flow solely depends on the primary shock Mach number or stronger primary shock (Eq. 34.1). Hence higher shock speed is the prime requirement for simulation of flows with higher stagnation temperature. Higher shock speeds can be achieved by incorporating convergence from driver section to driven section or by a convergent divergent diaphragm mounting station. Moreover the strength of the primary shock can be increased with increase in driver to driven gas pressure ratio and temperature ratio as shown in Eq. 34.4.

$$\frac{p_4}{p_1} = \frac{p_2}{p_1}\left[1 - \frac{(\gamma_4 - 1)\left(a_1 / a_4\right)\left(\left(p_2 / p_1\right) - 1\right)}{\sqrt{2\gamma_1}\left(\sqrt{2\gamma_1 + (\gamma_1 + 1)\left(\left(p_2 / p_1\right) - 1\right)}\right)}\right]^{\frac{-2\gamma_4}{(\gamma_4 - 1)}} \tag{34.4}$$

Operation of the shock tunnel with combustion driven shock tube (section 33.4) is one of the options for increase in driver to driven gas temperature ratio. The principle idea behind using combustion is with regard to driver gas heating. However there are numerous parallel ways investigated and reported in the literature. High enthalpy freestream can also be achieved in the test section by heating the driver gas of the shock tunnel by various methods viz. arc heating, shock heating and adiabatic compression of driver gas. Arc heating of the driver gas is achieved by installing electrodes in the driver section and string the arc across them. Thus generated arc deposits energy in the driver gas which in turn raises the driver gas temperature. The shock heating is carried out by using a double diaphragm shock tunnel. Schematic of the double diaphragm shock tunnel is as shown in **Fig. 34.2.** This operates like a conventional shock tunnel.

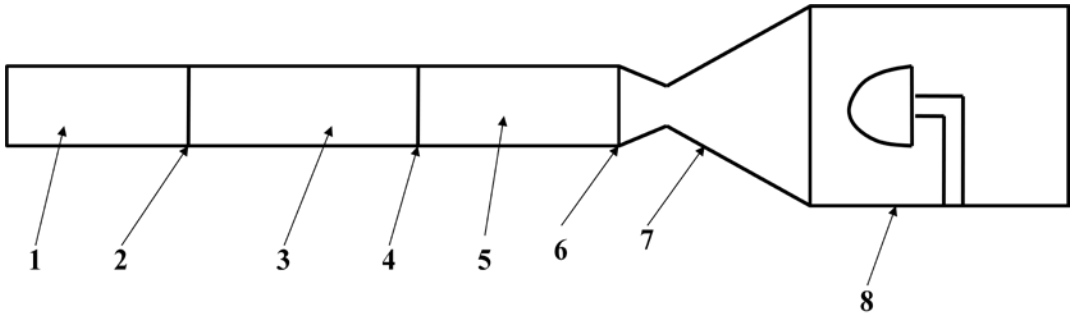

1. Primary Driver Section 2. Diaphragm 3. Main Driver Section 4.Diaphragm 5.Driven Section 6.Diaphragm 7.Nozzle 8.Test section and vacuum tank assembly

Fig. 34.2: Schematic of a typical double diaphragm shock tunnel.

This facility is same as that of shock tunnel. During the operation, all the diaphragms are mounted and required test gas is filled in the driven section. Low pressure is obtained in vacuum tank and driven gas pressure is set to the desired level. Main driver section is then filled with the main driver gas and pressure is noted. The primary driver section is then continuously filled with the driver gas. The driver gas filled in this section can be different from the one filled in the main driver section. Bursting of the diaphragm at station 2 (**Fig. 34.2**) starts the operation of the tunnel by initiating the shock in the main driver section. This shock increases the driver pressure and also heats it. Reflection of this shock further raises the driver pressure and temperature and bursts the diaphragm at station 4 (**Fig. 34.2**). Thus generated primary shock travels in the driven section. Further operation of the tunnel is same as that of the shock tunnel. This shock tunnel working methodology increases the primary shock strength and hence the nozzle supply conditions which makes this tunnel to be useful for wider range high enthalpy applications.

Lecture 35: Piston based shock Tunnels

35.1 Free-Piston Driven Shock Tunnel

This experimental facility also has its trait in the shock tube and hence has working principle similar to that of the shock tunnel. A typical free piston driven shock tunnel consists of a high pressure gas reservoir (secondary reservoir), piston, compression tube filled with driver gas, diaphragm, shock tube filled with driven gas or test gas, nozzle, test section and dump tank connected to a vacuum system. Schematic of a typical free piston driven reflected shock tunnel is shown in **Fig. 35.1**.

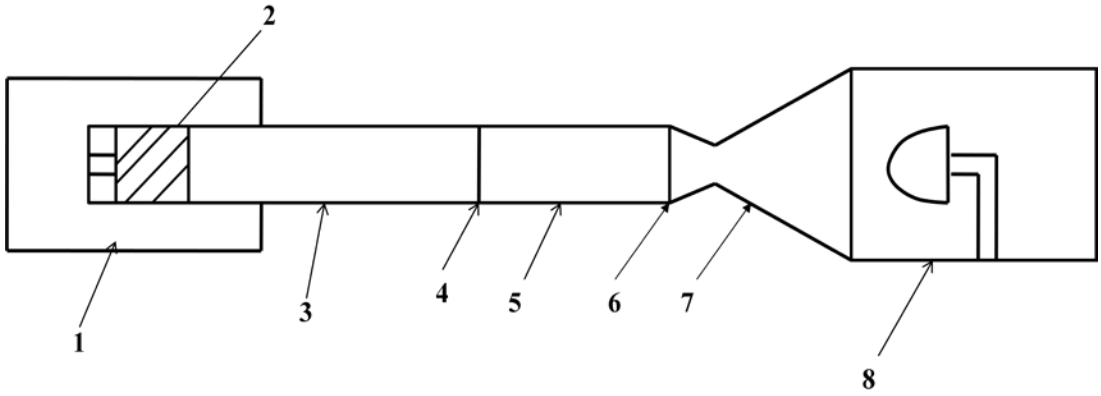

1. Secondary Reservoir 2. Piston 3. Compression tube 4. Diaphragm 5.Driven Section or shock tube 6.Diaphragm 7.Nozzle 8.Test section and vacuum tank assembly

Fig. 35.1: Schematic of a typical free piston driven shock tunnel.

Here secondary reservoir is separated by the piston from the compression tube. A metallic diaphragm separates the compression tube and shock tube or driven tube. The paper diaphragm (also called as secondary diaphragm) is mounted between shock tube and nozzle. Driver gas of required to the desired pressure level in the compression tube and the shock tube is filled with the test gas of at required pressure before conducting the experiment. Required vacuum is then obtained in the vacuum tank and test section part by using a high efficiency vacuum pump. During the experiment, sudden supply of the high pressure gas behind the piston sets it in motion in the compression tube. Motion of heavy piston in the compression tube adiabatically compresses the driver gas and in tern increases its pressure and temperature. This high pressure and high temperature driver gas ruptures the metallic or primary diaphragm. Rupture of the primary diaphragm produces a strong shock wave, which travels into

the driven section or the shock tube. This shock wave then reflects at end of the shock tube and provides high pressure and high temperature gas at the nozzle entry. Expansion of this gas through the nozzle produces the desired hypersonic flow in the test section of the free piston driven shock tunnel.

There are various challenges to operate the free-piston driven shock tunnel. Piston launch pressure in the secondary reservoir should be set judiciously so as to maintain constant pressure to drive the primary shock and also to ensure soft landing of piston at compression tube end. This adjustment of the piston launching pressure is termed as the ‘tuning operation’ where soft landing is achieved along with approximately constant driver pressure. Apart from the tuning operation, tailoring is also important to achieve the longer test duration. Test time of this tunnel is of the order of few milliseconds. Thus operated free-piston driven shock tunnel turns out to be an important experimental facility for high enthalpy or re-entry simulations.

35.2 Gun Tunnel

Configuration of a gun tunnel is similar to that of a free piston driven shock tunnel. This tunnel is also comprised of a driver gas reservoir, diaphragm, piston, test gas section or barrel, nozzle and test section cum dump tank. During the experiment, diaphragms are put in the respective locations and desired pressure is attained in the test gas section and dump tank. Continuous filling of the piston driver gas in the driver section bursts the diaphragm and the high pressure driver gas rushes in the barrel or driver section which sets piston in motion. Hence piston in the Gun Tunnel performs the same function as that of the contact surface and avoids the mixing of driver and driven gas. Thus attained motion of the piston compresses the test gas and also raises its temperature almost adiabatically. The main difference in Gun Tunnel and Free piston driven shock tunnel lies in that the piston compression is attained for the driver gas in the free piston driven shock tunnel while such is compression is obtained for the test gas in Gun Tunnel. Diaphragm at the nozzle inlet opens up at a particular test gas pressure and starts the expansion process in the nozzle. Thus expanded test gas attains hypersonic conditions in the Mach number. Gun Tunnel is very useful to obtain moderate stagnation enthalpy and high stagnation pressure hypersonic freestream in the test section.

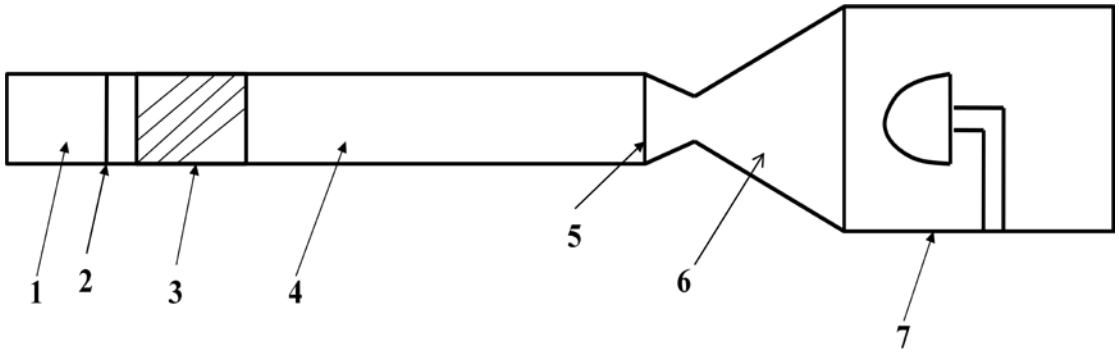

1. Driver Gas Reservoir 2. Diaphragm 3. Piston 4.Test gas section or Barrel 5.Diaphragm 6.Nozzle 7.Test section and vacuum tank assembly

Fig. 35.2 Schematic of a typical Gun Tunnel

35.3 Expansion Tube

Expansion tube is preferred for very high enthalpy or hypervelocity flows of the order 7 km/s and more. Free piston driven shock tunnel can also thought to use for such experiments but the disadvantage of this facility is that it provides dissociated freestream at the nozzle exit which is undesirable. This issue gets sorted by the use of expansion tube which provides hypervelocity freestream of air without dissociation. The lone disadvantage of this test facility is short test duration of the order of few tens of microseconds to few hundred microseconds. Schematic of this facility is as shown in **Fig.35.3**.

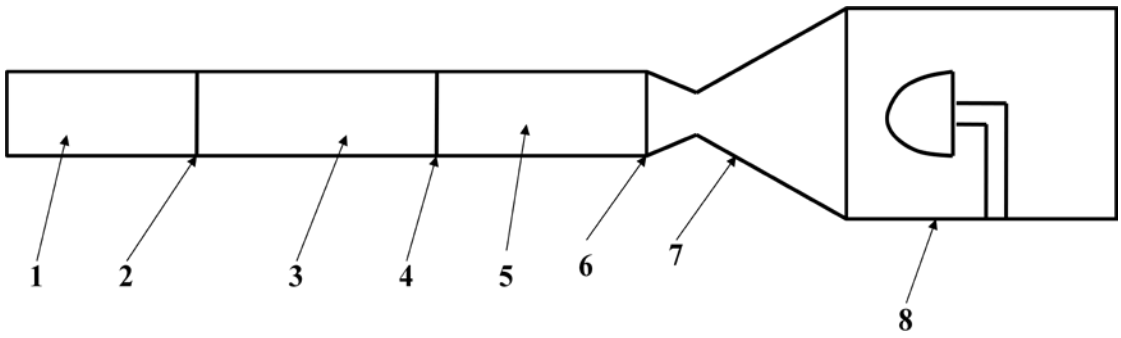

1. Driver Section 2. Diaphragm 3. Driven Section 4.Diaphragm 5.Acceleration tube 6.Diaphragm 7.Nozzle 8.Test section and vacuum tank assembly

Fig. 35.3: Schematic of a typical double diaphragm shock tunnel.

Operation of expansion tube is same as the shock tunnel. This test facility is comprised of three constant diameter tube sections separated by two diaphragms. These tubes are called as driver section, driven section and acceleration tube. This expansion tube part is connected with the tunnel portion and is separated by a paper diaphragm like the shock tunnel. Diaphragms are first mounted in the respective locations as a part of experimental preparation. Low pressure or vacuum is obtained in the test section cum dump tank portion using vacuum pump. Continuous filling of the driver gas in the driver section bursts the diaphragm and allows the high pressure driver to rush in the driven section. Thus generated primary shock sets motion for the driven or test gas and also raises its pressure and temperature. Passage of the primary shock bursts the diaphragm at location 4 (**Fig. 35.3**) since a light diaphragm is generally preferred at this location like the one used to separate the tunnel part from the tube. This diaphragm burst creates a shock which passes through the acceleration

tube and expansion waves which pass in the driven section. Driven or test gas speed increases in the presence of expansion waves. This unsteady expansion continues in the nozzle and test section where flow achieves hypervelocity test conditions. Various versions of the acceleration tube are possible which lead to enhance the speed to super-orbital speeds. Among those changes, use of double diaphragm shock tube, piston driven shock tube, compound shock tube etc are preferred ones to create the strong primary shock.

Lecture 36: Other hypersonic test facilities

36.1 Hot shot Tunnel

High enthalpy flows for long duration of few tens of milliseconds are generated using hot shock tunnel. This tunnel is comprised of an arc chamber with electrode arrangement which separates from the nozzle using a diaphragm. Nozzle exit is attached to a test section cum vacuum tank assembly. During the experiment very high amount of electrical energy is released in the arc chamber. This energy release heats the test gas in the arc chamber at constant volume and raises its temperature and pressure. Thus obtained pressure raise opens up the diaphragm at the nozzle inlet and sets the expansion of high pressure high temperature gas. Thus operated hot shot tunnel is capable of producing high enthalpy freestream in the test section.

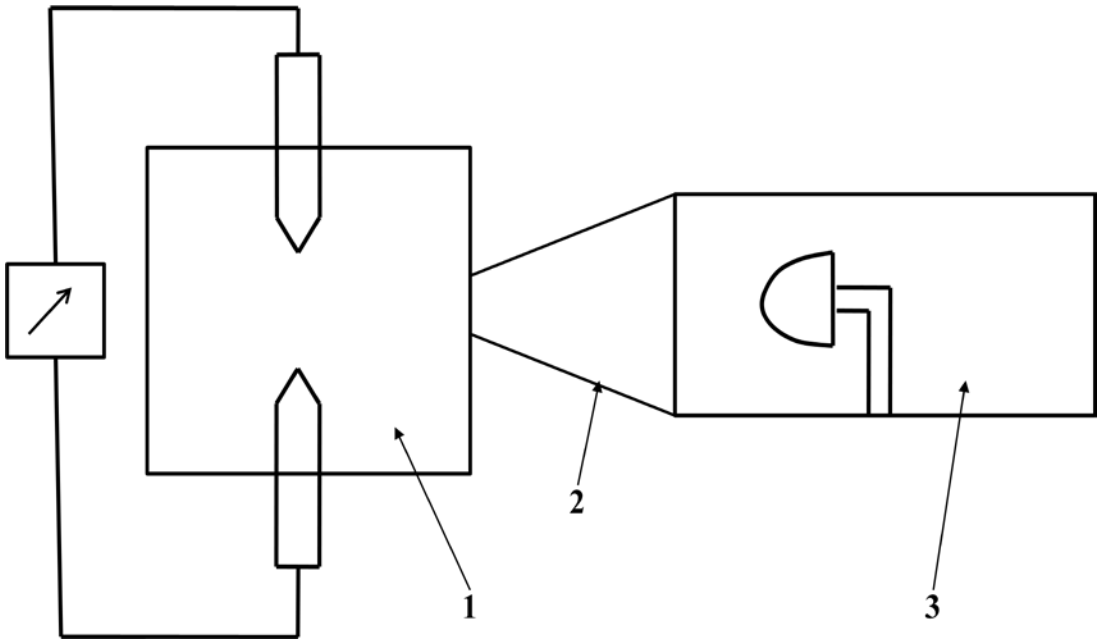

1. Arc chamber 2..Nozzle 3.Test section and vacuum tank assembly

Fig. 36.1: Schematic of a typical double diaphragm shock tunnel.

36.2 Launcher or Flight Test Facility

There are various types of launcher designs to study the hypersonic flight. Such a facility provides six degrees of freedom to the test models and also avoids the test gas contamination and dissociation which does match closely with the reality. A typical launcher is as shown in **Fig. 36.2.**

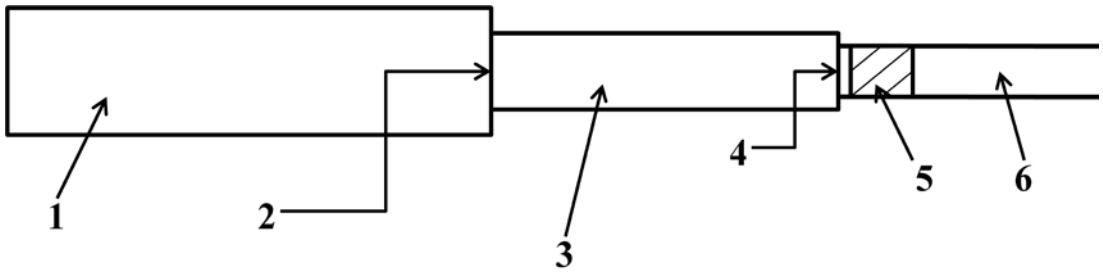

1. Driver Section 2. Diaphgram 3. Driven Section 4.Diaphragm 5.Test model 6. Launching barrel

Fig. 36.2: Schematic of a typical double diaphragm shock tunnel.

The driver section considered in this facility can also be combustion driver like a combustion driven shock tube. Operation of this facility is again similar to that of the double diaphragm shock tube. The bursting of second diaphragm, at location 4 (**Fig. 36.2**), sets the motion of the test object. Telemetry or optical systems are generally used to assist the desired measurements. Flight testing can also be achieved by using a gun powder which generates the blast wave after ignition and propels the object of interest. Standard launch vehicles can also be used for hypersonic flight testing based on the size of the test object.

Lecture 37: Heat transfer rate measurement

37.1 Heat transfer rate measurement

Knowledge of heat transfer rate is essential for the hypersonic flights for the design of thermal protection system. Hence heat transfer measurements are carried out in the experimental simulations. There are different sensors or methods for measuring the heat transfer rate which include thin film sensors and thermocouples. These sensors measure temperature time history during the experiment. This data is then used to estimate the local surface heat transfer rate.

37.1.1 Thin Film Sensors

This sensor is comprised of a substrate or backing material and sensing film. Various insulating materials like Macor, Pyrex glass etc. are available for the backing material. Macor (machinable ceramic) is used in experiments for heat transfer measurement, since it can be easily machined according to the curvature. Apart from the machinability, Macor is hard and brittle. Pyrex glass is preferred for configurations like flat plates. Both the backing materials can be used efficiently but their selection depends on the model to be tested. Thickness of the substrate is a very important element in the measurement of heat transfer rate since shape of the substrate is usually governed by the curvature of the test model. Moreover these sensors are flush mounted with the surface of test model to avoid any protrusion which affects the aerodynamic shape of the object. Knowledge of thickness of the substrate is necessary to estimate heat transfer rate from the experimentally obtained temperature signal using one dimensional heat conduction equation. Following assumptions are essential to predict the heat flux from temperature signal due to very small experimental duration.

1. Temperature measured by the sensing element is identical to the temperature at the substrate.
2. There is no lateral transfer of heat
3. Substrate is of infinite depth and temperature rise at infinity is zero.
4. Thermal properties of the substrate are constant.

Considering these assumptions, the temperature sensed by the sensing element can be considered to the same as the temperature measured on the surface of the substrate. Therefore, the thickness of the substrate should be orders of magnitude greater than the thickness of the thermal sensor placed on the substrate. The assumption of infinite thickness of the substrate makes it obvious to have corresponding temperature change at that end to be zero.

Extreme care is needed while preparing the thermal sensor. The thin film sensors need to have low response time hence platinum or nickel sensing materials are primarily considered for short duration testing. There are different techniques available to deposit platinum on the substrate. Sputtering is one among them and used to make the platinum thin films of required thickness. Hand painting of platinum paint on the substrate is also one of the easiest ways to make platinum thin films. The Macor strips are then put in the oven for baking which is then followed by natural cooling of the gauges. Silver paste is generally used to establish the required electrical connection to complete the fabrication of the thermal sensor. Schematic of a typical thermal sensor is shown in **Fig. 37.1**.

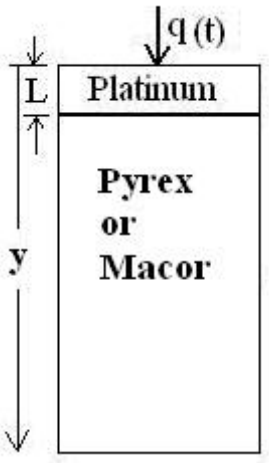

Fig. 37.1 Schematic of a typical thin film sensor

Thermal coefficient of resistance (TCR) should be measured for the fabricated thermal sensor. Typical experimental set up for the same is as shown in **Fig. 37.2**. This setup comprises of an empty beaker kept in oil filled beaker. The heat transfer gauge is placed in the empty beaker along with a thermometer. Thermometer and the gauge are put at the same height, so that the thermometer gives the temperature corresponding to the height of the gauge. The gauge is connected with a constant current source and a voltmeter is connected across the gauge to measure the voltage of

the gauge for the corresponding change in temperature. The oil bath is heated from the room temperature to maximum temperature of 90^0C. Then the process of heating is stopped and the bath is allowed to cool. The corresponding voltage readings are recorded at an interval of around 5^0C, while heating and cooling of the oil bath. From these readings, TCR (α) is obtained by the equation

$$\alpha = \frac{[\Delta V]}{[V_0 \Delta T]}$$

Here, V_0 is the initial voltage measured from initial resistance of the gauge and constant current and ΔV is the change in voltage for a change in temperature ΔT.

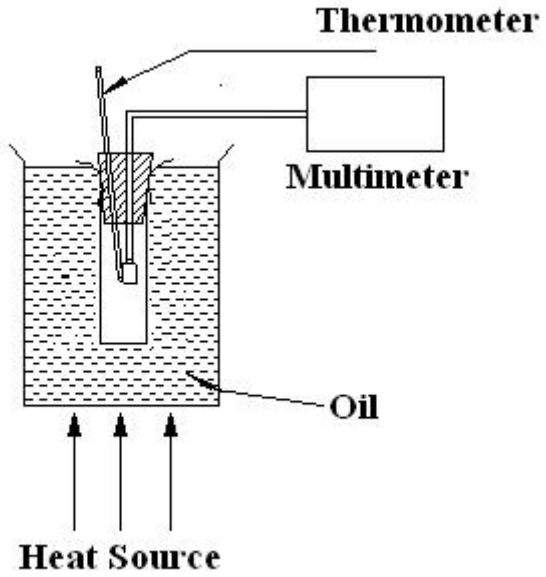

Fig. 37.2 Schematic of the experimental set-up for TCR estimation

37.1.2 Thermocouple

Thermocouple is a thermally active junction of two distinct metals which produce the voltage due to the temperature difference. Working principle of thermocouple is based on the Seebeck effect. Typical thermocouple circuit is as shown in **Fig. 37.3.**

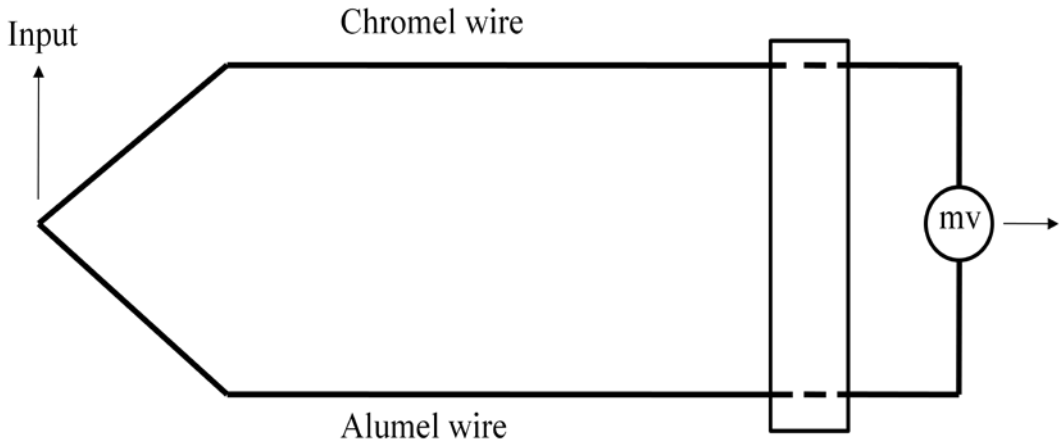

Fig. 37.3 Schematic diagram of the thermocouple

Response time of the thermocouple strongly depends on the junction properties. Hence coaxial thermocouples are generally preferred for hypersonic flow regime. However, thermocouples of type E and K are preferred for heat transfer rate measurements. Thermocouple of type E is comprised of chromel and constantan materials while type K is comprised of alumel and chromel. During fabrication of the co-axial thermocouple one thermocouple element is allowed to cover the other element while a thin electrical insulation separates them. The thermocouple junction is then formed by formal grinding or by polishing using the sandpaper. This process forms the junction at the microscopic level. Thus fabricated thermocouple is as shown in **Fig. 37.4.**

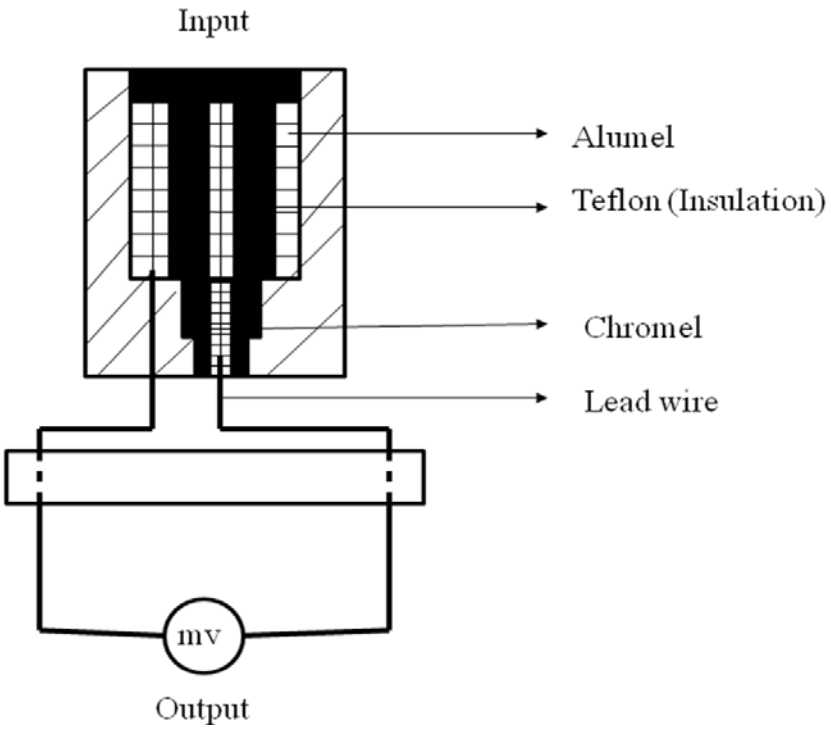

Fig 37.4 Schematic diagram of coaxial thermocouple

37.2 Heat transfer rate prediction

The time history of voltage obtained from the gauge during the experiment is used to find the heat transfer rate with the help of gauge material and backing material properties. The principle of unsteady 1D heat conduction is useful for these calculations of heat transfer rate. The gauge (platinum/nickel) deposited on the backing material or substrate has thickness in microns. This thickness can be assumed to be negligible in comparison with any other dimension of the gauge. Hence the governing equation is the unsteady heat conduction equation for the typical gauge geometry shown in **Fig. 37.5**.

From $0 \le y \le \infty$; $$\frac{\partial T}{\partial t} = \left(\frac{k}{\rho c_p} \right) \frac{\partial^2 T}{\partial y^2} \qquad (7.2)$$

The boundary conditions that are used (for both the regions) to solve the equation are, as follows,

For platinum material region,

At y = 0 (at the gauge surface); $t \le 0$, T = 0;

t > 0, $$\left(\frac{\partial T}{\partial y} \right)_{y=0} = -\frac{1}{k_1} q(t)$$

Here, k_1 is the thermal conductivity of gauge or sensing material (platinum), and q(t) is the heat transfer rate at the gauge location. If 'L' is the gauge thickness, then the boundary conditions for the backing material (Pyrex glass) region are

$t \le 0$; T = 0,

t > 0, y = L: $T_1(L)=T_2(L)$, $$k_1 \left(\frac{\partial T}{\partial y} \right)_{y=L} = k_2 \left(\frac{\partial T}{\partial y} \right)_{y=L}$$

k_1 and k_2 are the thermal conductivities of region 1 and 2 respectively. It signifies that the temperature of both the materials at the interface is same and the heat transferred by one material will be gained by other without any loss.

Lim y→∞, T=0.

Theory of Laplace Transform can be used to obtain the expression for heat flux from the temperature signal as given by Cook and Felderman (1966)

$$q(t) = \frac{\beta}{\sqrt{\pi}\alpha E_f}\left[\frac{E(t)}{\sqrt{t}} + \frac{1}{2}\int_0^t \frac{E(t)-E(\tau)}{(t-\tau)^{3/2}}\,d\tau\right]$$

Here E is the voltage, E_f is initial voltage, α is thermal coefficient of resistance of gauge material and backing material property is β.

Reference:

Cook W. J. and Felderman E.J. "Reduction of data from thin film heat transfer gauges: a concise numerical technique" AIAA J. Vol. 4. No 3, 1966, pp 561-562.

Lecture 38: Force measurement

38.1 Force measurement

Measurement of forces is useful for determination of aerodynamic coefficients, which in turn is useful for determination of fuel requirement of space vehicle and also for stability prediction. However, the measurement of forces in short duration facilities or at high enthalpy test conditions is difficult task. Several research groups have recently made the progress in designing force balances useful in flows of duration as short as one-millisecond. All these techniques for measurement of aerodynamic forces in impulse facilities are based on the use of either 1) force transducers 2) strain gauges and 3) accelerometers. Efforts are also put to measure the pressure at various locations on the object of interest to predict the force and moment. Some of the important and widely accepted techniques are discussed here.

38.2 Accelerometer Force Balance

Use of accelerometers for the measurement of force was initially proposed by Vidal (1956). Accelerometer based force balance is considered as the inertial dominated force balance. The general theory of a three component force balance and its application is briefly mentioned here. The spring mass concept is used to build this force balance. Therefore, the model and support system which experience the time dependant force are replaced by equivalent spring-mass system. The schematic of such a system, for a generic hypersonic configuration is shown in Fig. 38.1. The following assumptions have been made while designing the proposed system

(a) The springs are linear and they do not restrain lateral motion.
(b) There is no damping in the system.
(c) The axial force acts only through the center of gravity (*C.G*) of the model.
(d) Both the axial and normal forces vary with time.
(e) There are no coupling effects of axial and normal forces.

Let *m, J* and *I* be the mass, mass moment of inertia and the weight moment of inertia (*J=I/g*) of the model being used, respectively and K_1, K_2, K_3 be the spring constants being used. Consider three degrees of freedom to the test model due to the hypersonic flow over it in *x, y* and θ directions. Let *N(t)* be the normal force acting at the center of pressure at a distance *e* from the C.G of the model and *C(t)* be the axial force. Then, the model and the springs K_1 and K_2 constitute two degrees of freedom system with combined rectilinear and angular motion. The spring K_3 with the model constitutes a single degree of freedom system with a linear motion. The Newton's second law, the force in y direction can be written as:

$$m\ddot{y} = N(t) - K_1(y + a\theta) - K_2(y - b\theta)$$

Rearranging the above equation we get,

$$N(t) = m\ddot{y} + (K_1 + K_2)y + (aK_1 - bK_2)\theta$$

Similarly for x-direction force balance and moment we have,

$$C(t) = m\ddot{x} + K_3 x$$

$$J\ddot{\theta} = N(t)\cdot e - K_1(y + a\theta)a + K_2(y - b\theta)b$$

The boundary conditions for the equations (3.1), (3.2) and (3.3) are the following:

t≤0, N=0, C=0.

t>0, N=N(t), C=C(t).

The above equations with the boundary conditions can be solved using Laplace transform. Then, the solution for the accelerations works out to be as follows:

$$\ddot{y} = \left(\frac{N(t)}{m}\right)\left\{1 - t^2\left[\left(\frac{K_1 + K_2}{m}\right) + \left(\frac{e(aK_1 - bK_2)}{J}\right)\right]\right\}$$

$$\ddot{\theta} = \left(\frac{eN(t)}{J}\right)\left\{1 - t^2\left[\left(\frac{aK_1 - bK_2}{em}\right) + \left(\frac{a^2K_1 + b^2K_2}{J}\right)\right]\right\}$$

$$\ddot{x} = \left(\frac{C(t)}{m}\right)\left[1 - t^2\left(\frac{K_3}{2m}\right)\right]$$

The unknown forces (*N(t) and C(t)*) can be determined from above equations using the experimentally measured accelerations. The spring constants K_1, K_2 and K_3 appear as the coefficients of t^2 in the equations. The terms containing the product of time and spring constants become negligibly small for the test duration of few milliseconds

Therefore, assuming the model to be totally unrestrained during the test time in the shock tunnel, the above set of equations can be rewritten as,

$$N(t) = m\ddot{y}$$

$$N(t) = \ddot{\theta}\left(\frac{J}{e}\right)$$

$$C(t) = m\ddot{x}$$

It is necessary to measure the three accelerations $\ddot{y}, \ddot{\theta}, and\ \ddot{x}$ to determine the aerodynamic load. However measurement of the angular acceleration $\ddot{\theta}$ and the linear normal acceleration $\ddot{y}$, can be replaced by two linear accelerations which further can be added and subtracted to same effect as

$$\ddot{y} = \frac{b'\xi_1 + a'\xi_2}{a'+b'}$$

$$\ddot{\theta} = \frac{\xi_1 - \xi_2}{a'+b'}$$

The acceleration along the axis of the model is:

$$\ddot{x} = \xi_3$$

where, ξ_1, ξ_2 and ξ_3 are the accelerations measured by the front lift, aft lift and axial force accelerometers respectively mounted ahead and behind the center of gravity of the test model. Thus, the axial force and the normal force acting on the model can be written in terms of the measured accelerations as,

$$C(t) = m\xi_3$$

$$N(t) = \left[\frac{m}{a'+b'}\right](b'\xi_1 + a'\xi_2)$$

The aerodynamic drag coefficient C_d and lift coefficient C_L are computed using the relations,

$$C_d = \left(C(t)/(q_\infty S)\right)\cos\alpha + \left(N(t)/(q_\infty S)\right)\sin\alpha$$

$$C_L = \left(N(t)/(q_\infty S)\right)\cos\alpha - \left(C(t)/(q_\infty S)\right)\sin\alpha$$

This concept can be further stretched for measurement of six components.

38.2 Stress wave force balance

Sanderson and Simmons (1991) developed this technique for measuring a single component of force. Madhat et. al (2007) then stretched the applicability of this balance for three degree of freedom system. This force balance is considered as stiffness dominated force balance. It provides use of strain gauge to measure aerodynamic forces for test times of only a few milliseconds. Semiconductor strain gauges for high gauge factor are generally considered for this measurement. This balance, referred as the stress wave force balance, is based on the interpretation of transient stress waves propagating within the model and support during the test time. Upon establishment of the flow about the model and during the useful test period, a large number of stress wave reflections occur within the model and sting. The resulting outputs of the strain gauges mounted on the sting are used for the estimation of time history of the force. Extensive calibration of the instrumented test model is prime requirement of this force measurement technique.

The test model and support system are assumed to behave as a linear dynamic system under sudden application of aerodynamic load. A typical linear dynamic system is shown bellow, where, u(t) is input or the applied load, y(t) is output (strain signal) and g(t) is the system response function or transfer function.

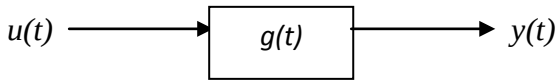

The relationship between input and output can be written as,

$$y(t) = \int_0^t g(t-\tau)u(\tau)d\tau$$

Time history of the applied aerodynamic load can be obtained by deconvolving the acceleration signal and the known system response function. Calibration of the force balance essentially gives the system characteristics in the form of the system response function. This calibration is carried out by monitoring the strain for the applied step or impulse load of known time variation. Convolution of the above equation for the known input and known out put gives the transfer function or system response function. For three degree of freedom system, the relation between the input and out put is as,

$$\begin{pmatrix} y_1 \\ y_2 \\ y_3 \end{pmatrix} = \begin{bmatrix} G_{11} & G_{12} & G_{13} \\ G_{21} & G_{22} & G_{23} \\ G_{31} & G_{32} & G_{33} \end{bmatrix} \begin{pmatrix} u_1 \\ u_2 \\ u_3 \end{pmatrix}$$

38.3 Other measurements at hypersonic speeds.

Pressure measurements are also carried out in the flow regime. However the pressure measurements are carried out using standard high response piezoelectric based pressure transducers. The flow diagnostic techniques considered in these facilities include the standard Schlieren and shadowgraph techniques.

References:

Madhat M.A, Mee D.J. and Morgan R.G., “New calibration technique for multi-component stress wave force balances.” Review of Scientific Instruments, 78, 065101, 2007.

Sanderson S. R., Simmons J. M., “Drag balance for hypervelocity impulse facilities.” AIAA Journal, 29 (12), 1991, pp. 2185-2191.

Vidal RJ, “Model instrumentation techniques for heat transfer and force measurements in a hypersonic shock tunnel.” Cornell Aeronautical Laboratory, Report WADC TN 56-315, 1956.